

# Fetal Lung Maturity Analysis using Sonogram Textural Features

K. N. Bhanu Prakash, A. G. Ramakrishnan, S. Suresh\*, and Teresa W P Chow<sup>#</sup>

Biomedical Lab., Dept. of Electrical Engg, Indian Institute of Science, Bangalore. Email: bhanu@ee.iisc.ernet.in

\* Fetal Care Research Foundation, Madras, India.

<sup>#</sup> Dept of O & G, University of Malaya, Malaysia.

**ABSTRACT--** Fetal lung and liver tissues were examined by ultrasound in 240 subjects during 24 to 38 weeks of gestational age, in order to determine the relationship between the gestational age and the textural features of sonograms of fetal lung. A region of interest of 64 X 64 pixels was used for extracting textural features. Since the histopathology of the liver is claimed to remain constant with respect to gestational age, features from the lung region are compared with those of liver. Though the means of the features show a specific trend with respect to gestation age, the variance is too high to guarantee any clustering with respect to age. Out of 64 features extracted, only 12 were unique and the rest showed similar variation. The features, by themselves, do not unambiguously determine whether the fetal lung is mature or immature.

## 1. INTRODUCTION

Prediction of lung maturity is important in the management of high-risk pregnancies. If the lungs are mature to sustain the newborn with no respiratory support, then prolonging of pregnancy is not required. However if they are immature, then the risks and costs of prolonging pregnancy may have to be weighed, especially in settings with limited neonatal support. The development of fetal lung involves the biochemical component of surfactant production and the anatomic component of development of airways and alveoli. Anatomic development of fetal lung seems to be closely related to gestational age, while biochemical maturity can occur as early as 28 weeks or as late as term.

Methods for determining fetal lung maturity include estimation of fetal size, gestational age, condition of placenta and biochemical tests on amniotic fluid. Though different properties of surfactants in amniotic fluid are studied, the L/S ratio remains the golden standard. All these tests necessitate amniocentesis, an invasive procedure that carries risks, and on occasion, may be contraindicated. Ultrasound cannot measure any of the biochemical parameters of fetal lung maturity, nor can it provide direct histologic information about fetal lung development. However, it is reasonable to assume that both morphological and biochemical changes alter the diffuse scattering and other propagation properties of fetal lung. This may change the textural appearance of sonogram. Sonographically determined parameters of fetal biparietal diameter and placental grading have been related to fetal maturity, with accuracy ranging from 78% to 100%.

Based on sonographic studies, Meyer [1] stated that the reflectivity of lung is equal to or less than that of the liver throughout most of pregnancy but this relationship reverses in late gestation. However, Cayea *et al.* [2] concluded that there is no statistically significant correlation between the sonographic features and biochemical fetal lung maturity indices (L/S ratio and PG values). Using RF signal for characterizing fetal lung and liver tissues, Benson *et al.* [3] inferred that there is a spectral shift from higher frequency content to lower frequency content when the fetal lung makes the transition from immature to mature state. Feingold *et al.* [4] used densitometer measurements to correlate lung–liver echogenicity with L/S ratio. Podobnik *et al.* [5] established a relation between coefficient of variation of lung–liver echogenicity and L/S ratio. In the present study, we tried to estimate gestation age by using textural features of the sonogram.

## 2. MATERIALS AND METHODS

Ultrasound examinations were performed using the real time, ATL Apogee 800 plus scanner with a 3.5 MHz curvilinear, broad bandwidth transducer probe with the dynamic range set at 55dB. The overall gain was set at an optimal value to get uniform visibility. The appropriate section was frozen and the image was grabbed. Longitudinal and transverse sections of the fetal thorax and upper abdomen were imaged. The fetal lung and liver were identified in the thoracic and upper abdominal sections, respectively. Care was taken to avoid obvious vascular structures in the liver. Data was collected from 240 subjects at various gestation ages from 24 weeks to 38 weeks. Data were collected both at Mediscan Systems, Chennai and University Hospital in Kuala Lumpur, Malaysia. A region of interest of 64 X 64 pixels was used for extracting a number of quantitative parameters related to texture. The ratio of lung to liver feature was studied as possible index of maturity. The details of other features are given in the subsections 2.1 to 2.4.

## 2.1 Spatial Gray Level Dependence Matrices (SGLDM)

The SGLDM are based on the estimation of second order joint conditional probability density functions,  $f(i, j; d / \theta)$ . Here  $f(i, j; d / \theta)$  is the probability that a pair of pixels separated by a distance  $d$  at an angle  $\theta$  have gray levels  $i$  and  $j$ . The angles are quantized to  $45^\circ$  intervals. The estimated density functions, denoted by  $P(i, j; d / \theta)$  are defined as,

$$P(i, j; d, 0^\circ) = \# \{((k, l), (m, n)) \in (L_X \times L_Y) \times (L_Y \times L_X) : k - m = d, l - n = 0, I(k, l) = i, I(m, n) = j\} / T(d, 0^\circ)$$

$$P(i, j; d, 45^\circ) = \# \{((k, l), (m, n)) \in (L_X \times L_Y) \times (L_Y \times L_X) : (k - m = d, l - n = -d) \text{ or } (k - m = -d, l - n = d), I(k, l) = i, I(m, n) = j\} / T(d, 45^\circ)$$

$$P(i, j; d, 90^\circ) = \# \{((k, l), (m, n)) \in (L_X \times L_Y) \times (L_Y \times L_X) : |k - m| = d, l = n, I(k, l) = i, I(m, n) = j\} / T(d, 90^\circ)$$

$$P(i, j; d, 135^\circ) = \# \{((k, l), (m, n)) \in (L_X \times L_Y) \times (L_Y \times L_X) : (k - m = -d, l - n = -d, I(k, l) = i, I(m, n) = j) / T(d, 135^\circ)$$

where  $\#$  denotes the number of elements in the set,  $L_X$  and  $L_Y$  are the horizontal and vertical spatial domains,  $I(x, y)$  is the image,  $d$  is the inter-sample spacing and  $\theta$  is the direction angle.

Haralick [6] proposed 14 texture measures that can be extracted from the  $P(i, j; d, \theta)$  matrices. In our study, only the following five texture features [7] were computed.

$$\text{Energy} : E(S_\theta(d)) = \sum_{i=0}^{N_G-1} \sum_{j=0}^{N_G-1} [s_\theta(i, j | d)]^2 \quad \text{Entropy} : H(S_\theta(d)) = - \sum_{i=0}^{N_G-1} \sum_{j=0}^{N_G-1} s_\theta(i, j | d) \log s_\theta(i, j | d)$$

$$\text{Correlation} : C(S_\theta(d)) = \frac{\sum_{i=0}^{N_G-1} \sum_{j=0}^{N_G-1} (i - \mu_x)(j - \mu_y) s_\theta(i, j | d)}{\sigma_x \sigma_y}$$

$$\text{Inertia} : (S_\theta(d)) = \sum_{i=0}^{N_G-1} \sum_{j=0}^{N_G-1} (i - j)^2 s_\theta(i, j | d)$$

$$\text{Local Homogeneity} : L(S_\theta(d)) = \sum_{i=0}^{N_G-1} \sum_{j=0}^{N_G-1} \frac{1}{1 + (i - j)^2} s_\theta(i, j | d)$$

where  $s_\theta(i, j | d)$  the  $(i, j)^{\text{th}}$  element of  $S_\theta$ ,  $N_G$  is the number of gray levels in the image and

$$S_\theta(d) = P(I, j; d, 0^\circ); \quad S_{45}(d) = P(I, j; d, 45^\circ); \quad S_{90}(d) = P(I, j; d, 90^\circ); \quad \text{and} \quad S_{135}(d) = P(I, j; d, 135^\circ);$$

$$\begin{aligned} \mu_x &= \sum_{i=0}^{N_G-1} i \sum_{j=0}^{N_G-1} s_\theta(i, j | d) & \mu_y &= \sum_{j=0}^{N_G-1} j \sum_{i=0}^{N_G-1} s_\theta(i, j | d) \\ \sigma_x^2 &= \sum_{i=0}^{N_G-1} (i - \mu_x)^2 \sum_{j=0}^{N_G-1} [s_\theta(i, j | d)] & \sigma_y^2 &= \sum_{j=0}^{N_G-1} (j - \mu_y)^2 \sum_{i=0}^{N_G-1} [s_\theta(i, j | d)] \end{aligned}$$

## 2.2 The Gray Level Difference Matrix (GLDM)

Let  $I(x, y)$  be the image intensity function. For any given displacement  $\delta = (\Delta x, \Delta y)$ , let  $I_\delta(x, y) = |I(x, y) - I(x + \Delta x, y + \Delta y)|$  and  $f'(i | \delta)$  be the probability density of  $I_\delta(x, y)$ . If there are  $m$  gray values, this has the form of a  $m$ -dimensional vector whose  $i^{\text{th}}$  component is the probability that  $I_\delta(x, y)$  will have value  $i$ . The value of  $f'(i | \delta)$  is obtained from the number of times  $I_\delta(x, y)$  occurs for a given  $\delta$ , i.e.

$$f'(i | \delta) = P(I_\delta(x, y) = i)$$

Four possible forms of the vector  $\delta$  were considered:  $(0, d)$ ,  $(-d, d)$ ,  $(d, 0)$ , and  $(-d, -d)$ , where  $d$  is the interpixel distance. From each of these density functions, five texture features were extracted. They are:

$$\text{Contrast} : \text{CON} = \sum_{i=0}^{N_G-1} i^2 f'(i | \delta) \quad \text{Mean} = \sum_{i=0}^{N_G-1} i f'(i | \delta)$$

$$\text{Entropy: } ENT = \sum_{i=0}^{N_G-1} f'(i|\delta) \log(f'(i|\delta)) \quad \text{Inverse Difference Moment: } IDM = \sum_{i=0}^{N_G-1} \frac{f'(i|\delta)}{i^2 + 1}$$

$$\text{Angular Second Moment: } ASM = \sum_{i=0}^{N_G-1} [f'(i|\delta)]^2$$

### 2.3 Laws' Texture Energy Measures

Laws' texture energy measures [8] are derived from three vectors of length 3:  $L3 = (1, 2, 1)$ ,  $E3 = (-1, 0, 1)$  and  $S3 = (-1, 2, -1)$ , which represent the operations of local averaging, edge detection and spot detection. If these vectors are convolved with themselves or with one another, we obtain five vectors of length 5:  $L5 = (1, 4, 6, 4, 1)$ ,  $S5 = (-1, 0, 2, 0, -1)$ ,  $R5 = (1, -4, 6, -4, 1)$ ,  $E5 = (-1, -2, 0, 2, 1)$  and  $W5 = (-1, 2, 0, -2, 1)$  which perform local averaging, spot, ripple, edge and wave detection, respectively. The masks used in our analysis are  $L5 \text{ ' } E5$  and  $L5 \text{ ' } S5$ . After convolving with the masks, the energy of the resulting image was calculated.

### 2.4. Fractal dimension and Lacunarity

The above conventional methods measure the coarseness, directionality and energy. However, they do not consider an important characteristic, namely, the granularity. An intensity surface of an ultrasonic image can be viewed as the end result of random walks, and fractional Brownian motion model [9] can be used for its analysis. Fractal dimension and lacunarity are the important features that characterize the roughness and granularity of the surface.

Given an  $M \times M$  image  $I$ , the intensity difference vector is defined as  $IDV = [id(1), id(2), \dots, id(s)]$ , where  $s$  is the maximum possible scale and  $id(k)$  is the average of the absolute intensity difference of all pixel pairs with horizontal or vertical distance  $k$ . We compute  $id(k)$  as

$$id(k) = \frac{\sum_{x=0}^{M-1} \sum_{y=0}^{M-k-1} |I(x, y) - I(x, y+k)| + \sum_{x=0}^{M-k-1} \sum_{y=0}^{M-1} |I(x, y) - I(x+k, y)|}{2M(M-k-1)}$$

and  $D = 3 - H$ , where  $D$  is the fractal dimension. The value of  $H$  is obtained by using least-squares linear regression to estimate the slope of the curve of  $id(k)$  versus  $k$  in log-log scale. Given a fractal set  $A$ , let  $P(m)$  be the probability that there are  $m$  points within a box of size  $L$ , centered about an arbitrary point of

$A$ . We have  $\sum_{m=1}^N P(m) = 1$ , where  $N$  is the number of possible points within the box. The lacunarity is

$$\text{defined as } \Lambda = \frac{(M_2 - M^2)}{M^2}, \quad \text{where } M = \sum_{m=1}^N mP(m) \text{ and } M_2 = \sum_{m=1}^N m^2 P(m)$$

## 3. RESULTS AND DISCUSSION

Out of the 64 features extracted, only 12 features were found unique and the rest were redundant. Since the features of SDLM and SGLDM had similar variations, and computation of SGLDM features is both time and memory consuming, we discarded SGLDM features. The features selected were: fractal dimension and lacunarity from fractal measures, contrast, angular second moment, entropy, mean, inverse difference moment from SDLM, energy measures from laws' textural masks and mean, variance and coefficient of variation from histogram of the image. Min-max normalization was used to normalize the feature values. The variation of lung – liver feature is shown in Fig. 1 and the variations of different features of lung and liver regions are shown in Fig. 2. Data sets from both hospitals had similar behaviour.

## 4. CONCLUSIONS

Based on the data analyzed and the features studied, it appears that an unambiguous decision about fetal lung maturity cannot be made purely based on the characteristics of the ultrasound images.

## 5. BIBLIOGRAPHY

- [1] Johnson Meyer, Silvers Herron, Thieme, Banjavic and Carson. "Sonographic identification of lung maturation in the fetal lamb" *Invest. Radiology*, 1983; vol 18, page 18 -26.
- [2] Grant D.C., Doubilet P.M., Jones.T.B and Cayea P.D. "Prediction of fetal lung maturity: inaccuracy of study using conventional ultrasound instruments" *Radiology*, 1985; vol 155, page 473--475.
- [3] D.M. Benson and L.D. Waldroup "Ultrasonic tissue characterization of fetal lung, liver and placenta for the purpose of assessing fetal maturity" *Jl of Ultrasound in Medicine*, 1983; vol 2, page 489--494.

- [4] Michael Feingold, James Scollins, Curtis Cetrulo, and Douglas Koza. "Fetal lung to liver reflectivity ratio and lung maturity". *Journal of Clinical Ultrasound*, 1987; vol. 15, page 384--387.
- [5] M.Podobnik, B.Brayer, and B.Ciglar. "Ultrasonic fetal and placenta tissue characterization and lung maturity". *International Journal of Gynecology and Obstetrics*, 1996; vol. 54; page 221--229.
- [6] RM Haralick "Statistical and structural approaches to texture", *Proc.IEEE*, 1979, vol67(5), p.304-322.
- [7] R.W.Conners and CA.Harlow "A theoretical comparison of texture algorithms". *IEEE Trans. PAMI*, 1980; vol. 2(3): p. 204--222.
- [8] K.I.Laws. "Texture energy measures". *Proc. Image understanding Workshop*, 1979; pages 47--51.
- [9] J.M.Keller, S.Chen, and Crownover. "Texture description and segmentation through fractal geometry". *Computer Vision, Graphics and Image Processing*, 1989;vol 45: page 150--166.

Fig. 1. Variation of mean ratio of lung-liver features with respect to gestational age.

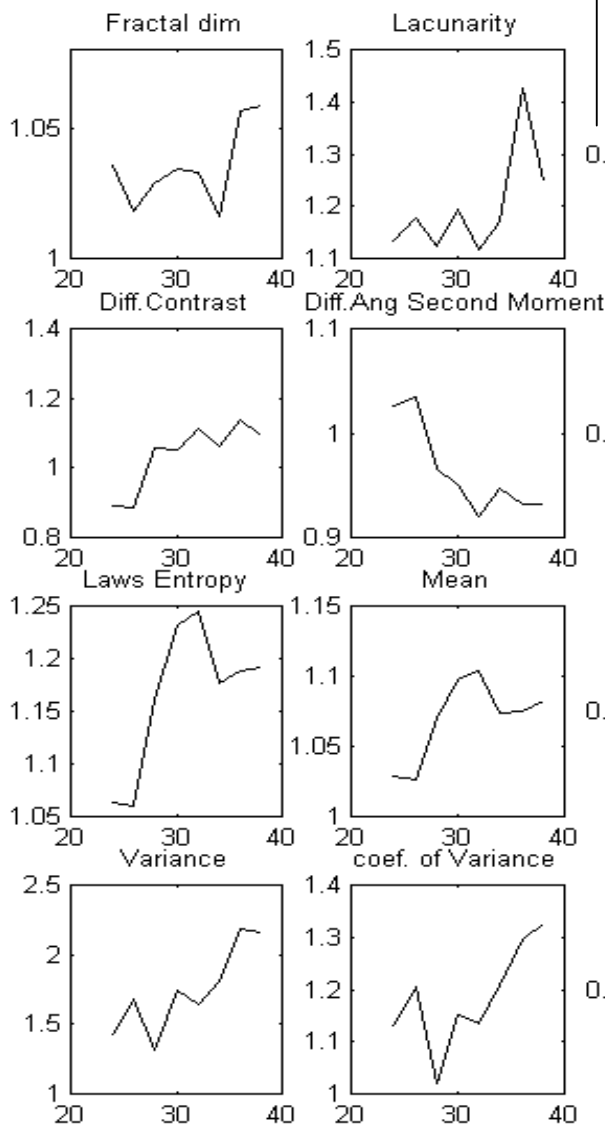


Fig. 2. Variation of mean (n=30) of the various features with respect to gestational age. (--- liver; — lung)

